

TREM2 sustains microglial expansion during aging and response to demyelination

Pietro Luigi Poliani,¹ Yaming Wang,² Elena Fontana,¹ Michelle L. Robinette,² Yoshinori Yamanishi,² Susan Gilfillan,² and Marco Colonna²

¹Department of Molecular and Translational Medicine, Pathology Unit, University of Brescia School of Medicine, Brescia, Italy. ²Department of Pathology and Immunology, Washington University School of Medicine, St. Louis, Missouri, USA.

Microglia contribute to development, homeostasis, and immunity of the CNS. Like other tissue-resident macrophage populations, microglia express the surface receptor triggering receptor expressed on myeloid cells 2 (TREM2), which binds polyanions, such as dextran sulphate and bacterial LPS, and activates downstream signaling cascades through the adapter DAP12. Individuals homozygous for inactivating mutations in *TREM2* exhibit demyelination of subcortical white matter and a lethal early onset dementia known as Nasu-Hakola disease. How TREM2 deficiency mediates demyelination and disease is unknown. Here, we addressed the basis for this genetic association using *Trem2*^{-/-} mice. In WT mice, microglia expanded in the corpus callosum with age, whereas aged *Trem2*^{-/-} mice had fewer microglia with an abnormal morphology. In the cuprizone model of oligodendrocyte degeneration and demyelination, *Trem2*^{-/-} microglia failed to amplify transcripts indicative of activation, phagocytosis, and lipid catabolism in response to myelin damage. As a result, *Trem2*^{-/-} mice exhibited impaired myelin debris clearance, axonal dystrophy, oligodendrocyte reduction, and persistent demyelination after prolonged cuprizone treatment. Moreover, myelin-associated lipids robustly triggered TREM2 signaling in vitro, suggesting that TREM2 may directly sense lipid components exposed during myelin damage. We conclude that TREM2 is required for promoting microglial expansion during aging and microglial response to insults of the white matter.

Introduction

Triggering receptor expressed on myeloid cells 2 (TREM2) is a cell-surface receptor of the Ig superfamily that is found in microglia, osteoclasts, and other tissue macrophages in vivo (1–3) as well as in monocyte-derived DCs (4), bone marrow-derived macrophages, and macrophage cell lines in vitro (5). TREM2 binds polyanions, such as dextran sulphate, bacterial lipooligosaccharides, and various phospholipids (6–8). It transmits intracellular signals through an associated transmembrane adapter, DAP12, which contains tyrosine-based activation motifs (ITAMs) in its cytoplasmic domain (9). DAP12 ITAMs recruit the protein tyrosine kinase Syk, which mediates the phosphorylation of PLC- γ , PI3K, Vav2/3, and other downstream molecules that trigger cell activation (10). Besides directly triggering tyrosine phosphorylation, the TREM2/DAP12 complex cooperates with CSF-1 receptor (CSF-1R) signaling (11), while it interferes with TLR signaling (12–14).

Individuals homozygous for rare inactivating mutations in either *TREM2* or *TYROBP*, which encodes DAP12, develop a lethal form of progressive, early onset dementia known as Nasu-Hakola disease (NHD) (1). Patients with NHD are asymptomatic through early adulthood, present with neuropsychiatric symptoms in their third and fourth decades, and expire between the ages of 35 and 45 (15). Postmortem analysis of these rare

patients has revealed massive gliosis, with pathology predominantly of the subcortical white matter that includes common demyelinating lesions (15).

While generation of myelin depends primarily on oligodendrocytes (ODCs) (16), microglia contribute to myelination by removing damaged myelin sheaths and releasing soluble factors that promote differentiation of ODCs and subsequent remyelination (17–19). Thus, the association between TREM2 deficiency and demyelinating NHD suggests that microglia may require TREM2 for removing damaged myelin and supporting myelin regeneration by ODCs. While DAP12-deficient mice showed thalamic hypomyelination with synaptic degeneration (20), the function of TREM2 in myelination remains to be directly investigated. An in vitro study found that reduced expression of TREM2 in a microglia cell line impaired phagocytosis of apoptotic neurons (21). Moreover, an in vivo study showed that intravenous injection of bone marrow-derived myeloid cells overexpressing TREM2 during experimental autoimmune encephalomyelitis, a model of immune-mediated demyelination, curbed disease by promoting the clearance of apoptotic neurons and secretion of IL-10 (22). However, this model may not recapitulate the function of bona fide microglia, either in normal myelination or nonautoimmune demyelinating diseases, such as NHD. In fact, microglia are brain-resident cells that populate the brain during embryogenesis and self renew throughout life (23–25), whereas adoptively transferred myeloid cells reach the CNS only when inflammation disrupts the blood-brain barrier (26).

Here, we addressed the impact of TREM2 deficiency on brain-resident microglia in vivo during aging and in a model of

Authorship note: Pietro Luigi Poliani and Yaming Wang contributed equally to this work.

Conflict of interest: The authors have declared that no conflict of interest exists.

Submitted: July 14, 2014; **Accepted:** March 17, 2015.

Reference information: *J Clin Invest*. 2015;125(5):2161–2170. doi:10.1172/JCI77983.

nonautoimmune demyelination, the cuprizone model, which is characterized by apoptosis of mature ODCs, followed by recruitment of astrocytes and activation of brain-resident microglia to remove myelin debris (27, 28). We found that total numbers and density of microglia increased with age in various regions of the brain in WT mice, as previously reported (29–31), whereas age-matched *Trem2*^{-/-} mice had fewer microglia. After cuprizone challenge, *Trem2*^{-/-} microglia failed to activate transcriptional programs that promote myelin removal and repair, such as lipid/fatty acid capture, transport, and metabolism, as well as those encoding chemoattractants, inflammatory mediators, and trophic factors for ODCs. Impaired microglial activation was associated with prolonged microgliosis, likely stimulated by persistence of myelin debris, as well as impaired repopulation of ODCs and subsequent remyelination. Moreover, a TREM2 reporter assay showed that TREM2 detects lipidic components of myelin, suggesting that TREM2 directly senses myelin damage. We postulate that TREM2 is a lipid sensor that is essential to promoting microglial activation in response to insults to the white matter.

Results

TREM2 deficiency affects microglial numbers during aging. NHD becomes clinically apparent in presenile individuals, and the underlying pathological changes are recorded postmortem. However, it is not known at which point in life TREM2 deficiency begins to affect microglia and myelination. To address this question, we stained brain sections of 6-month-old, 1-year-old, and 2-year-old WT and *Trem2*^{-/-} mice for ionized calcium-binding adapter molecule 1 (Iba-1), which is a marker commonly used to identify microglia in the CNS. WT mice had a progressive increase in microglia over time, which was highly significant in the white matter, particularly in the corpus callosum ($P < 0.0001$) and the cerebellum ($P < 0.01$), but not in the cerebral cortex (Figure 1, A and B). Although *Trem2*^{-/-} mice showed microglial numbers similar to WT mice at 6 months, no obvious increase occurred over time. In fact, microglia were significantly less abundant in 2-year-old *Trem2*^{-/-} mice than in age-matched WT mice, especially in the corpus callosum, cerebellum, and hippocampus ($P < 0.0001$, $P < 0.01$, $P < 0.05$) (Figure 1, A and B). Additionally, microglia in 2-year-old *Trem2*^{-/-} mice showed dystrophic morphology characterized by smaller cell body and reduced ramifications (Figure 1B, insets, and Figure 1C). Measurement of Iba-1⁺ areas confirmed a progressive shrinking of the cell body of TREM2-deficient microglia (Figure 1D). Thus, TREM2 deficiency affects long-term numbers and morphology of microglia. These results are reminiscent of those we previously reported for microglia in 1-year-old *Dap12*^{-/-} mice, which are present in lower numbers and have abnormal morphology compared with WT mice (11). Despite microglial defects, TREM2 deficiency was not associated with marked demyelination, neuronal loss, other marked histological changes, or obvious behavioral abnormalities in aged mice (data not shown), suggesting that a deficit of TREM2 in mouse is not sufficient to cause pathological changes equivalent to human NHD.

TREM2 is required for myelin debris removal and remyelination after cuprizone-induced demyelination. As *Trem2*^{-/-} mice did not develop spontaneous demyelination, we wanted to determine

whether TREM2 deficiency increases susceptibility to induced demyelination. To address this question, we chose to study the cuprizone model of demyelination, in which cuprizone exposure induces apoptosis of mature ODCs, demyelination in the CNS, recruitment of astrocytes, and activation of brain-resident microglia without damaging the blood-brain barrier (27, 28). In this model, there is no confounding infiltration of bone marrow-derived myeloid cells (26, 32). WT and *Trem2*^{-/-} mice were fed a diet containing 0.2% cuprizone. Mice were analyzed at 4 weeks, the peak of demyelination, or at 12 weeks, at which point both demyelination and remyelination occur. Some groups of mice were fed a normal diet for 2 additional weeks after 4 or 12 weeks of cuprizone treatment to allow myelin recovery. We analyzed myelination of untreated, cuprizone-treated, and recovering mice by transmission electron microscopy (TEM) of the corpus callosum, a sensitive target of demyelination. To precisely quantify the extent of demyelination and remyelination, we measured the ratio of axon circumference to myelin circumference (G ratio). Before cuprizone exposure, the corpus callosum of *Trem2*^{-/-} mice was myelinated to the same extent as that in the WT mice (Figure 2, A–C). After 4 weeks of cuprizone treatment, WT mice showed clear demyelination, with axonal swelling, increased G ratio, and accumulation of myelin debris (Figure 2, A–C). Myelination returned to normal after 2 weeks of a cuprizone-free diet (Supplemental Figure 1; supplemental material available online with this article; doi:10.1172/JCI77983DS1). Like WT mice, *Trem2*^{-/-} mice showed a clear demyelination at 4 weeks (Figure 2, A–C), which was repaired after 2 weeks of a cuprizone-free diet (Supplemental Figure 1). After 12 weeks of cuprizone treatment, WT mice showed partial demyelination, suggesting ongoing remyelination, which became complete after 2 weeks of a cuprizone-free diet (Figure 2, A–C). In contrast, the corpus callosum of *Trem2*^{-/-} mice remained largely demyelinated and showed abundant accumulation of myelin debris, which persisted even after the 2-week recovery period (Figure 2, A–C). *Trem2*^{-/-} mice showed clear axonal dystrophy, as evinced by the presence of axonal spheroids and increased G ratio throughout the experiment (Figure 2C). These data indicate that TREM2 deficiency has no impact on the initial demyelination, but does affect subsequent remyelination when the cuprizone treatment is prolonged, most likely by impairing myelin removal as well as myelin regeneration.

To corroborate these results, we performed immunohistochemical analysis of myelin basic protein (MBP), a major component of myelin. WT mice showed an initial reduction of MBP staining after 4 weeks of cuprizone treatment, followed by a sharp reduction after 12 weeks and a reconstitution of a normal MBP staining in the recovery phase (Figure 2, D and E). We interpret the MBP reduction at 4 weeks to reflect apoptosis of myelinating ODCs, whereas the sharp MBP reduction at 12 weeks was probably due to the removal of damaged myelin. In *Trem2*^{-/-} mice, MBP staining also appeared reduced at 4 weeks to levels similar to those of WT, but unlike in WT mice, the sharp reduction in MBP staining was not apparent at 12 weeks and MBP continued to be reduced after 2 weeks of recovery. These data corroborate that TREM2 deficiency results in impaired clearance of damaged myelin after prolonged demyelination,

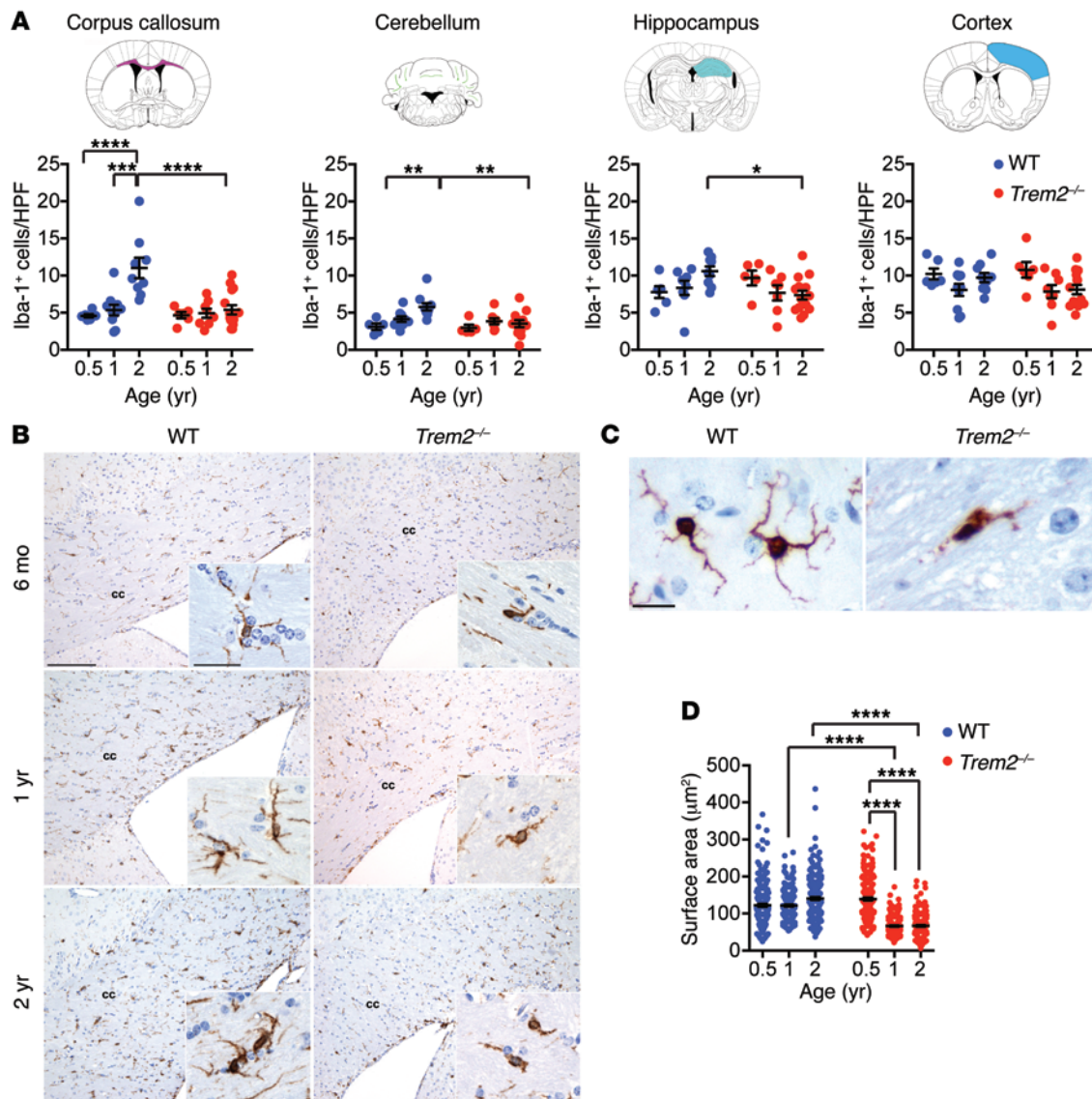


Figure 1. *Trem2* deficiency affects aging-dependent expansion of microglia. (A) Microglial numbers were counted as Iba-1⁺ cells per high-power field (HPF) in the corpus callosum, cerebellum, hippocampus, and cortex in mice at 6 months, 1 year, and 2 years after birth. Brain regions analyzed are shown in the corresponding drawings. (B) Representative images of Iba-1⁺ cells in WT and *Trem2*^{-/-} mice at different ages. cc, corpus callosum. (C and D) Steady-state microglia in aged *Trem2*^{-/-} mice show deramified morphology compared with microglia of age-matched WT mice. (C) Representative images of Iba-1⁺ cells in 2-year-old WT and *Trem2*^{-/-} mice. (D) Quantification of microglial surface area (in μm^2) visualized by Iba-1 staining. * $P \leq 0.05$; ** $P \leq 0.01$; *** $P \leq 0.001$; **** $P \leq 0.0001$, 2-way ANOVA. Original magnification, $\times 20$ (B); $\times 60$ (B, insets; C). Scale bars: 100 μm (B); 30 μm (B, insets; C). Data represent 5 to 10 mice (A and B) and 4 mice (C and D) for each group from a total of 2 experiments. An average of 10 HPF per mouse were evaluated in A. An average of 50 cells in 10 HPF per mouse were evaluated in D. Error bars represent mean \pm SEM.

which hinders subsequent myelin regeneration. This conclusion was supported by immunohistochemical analysis of ODC. WT mice showed a limited reduction of ODCs after 4 and 12 weeks of cuprizone treatment, which stabilized during recovery, whereas *Trem2*^{-/-} mice showed a progressive and significant ODC reduction during cuprizone treatment and recovery (Figure 2, F and G). We conclude that prolonged treatment of *Trem2*^{-/-} mice with cuprizone causes a persistent demyelination that mimics that observed in NHD.

Trem2^{-/-} mice show dystrophic microgliosis in response to demyelination. We next sought to define the mechanism of defective remyelination in *Trem2*^{-/-} mice. Although TREM2 expression has

been reported in CNS cells other than microglia (33, 34), recently published studies demonstrated that *Trem2* is specifically expressed in microglia — but not other cells in the CNS — under steady-state conditions (35–37). Moreover, we found that *Trem2* was not expressed in astrocytes or ODC precursors after 4 weeks of cuprizone feeding, while its expression in microglia was elevated (Supplemental Figure 2). These data indicate that impact of TREM2 on remyelination is largely through microglia.

To investigate the microglial response to cuprizone-induced demyelination, we stained brain sections for Iba-1 and determined the frequency of Iba-1⁺ cells. Consistent with previous reports (38), WT mice showed a peak of microgliosis at 4 weeks

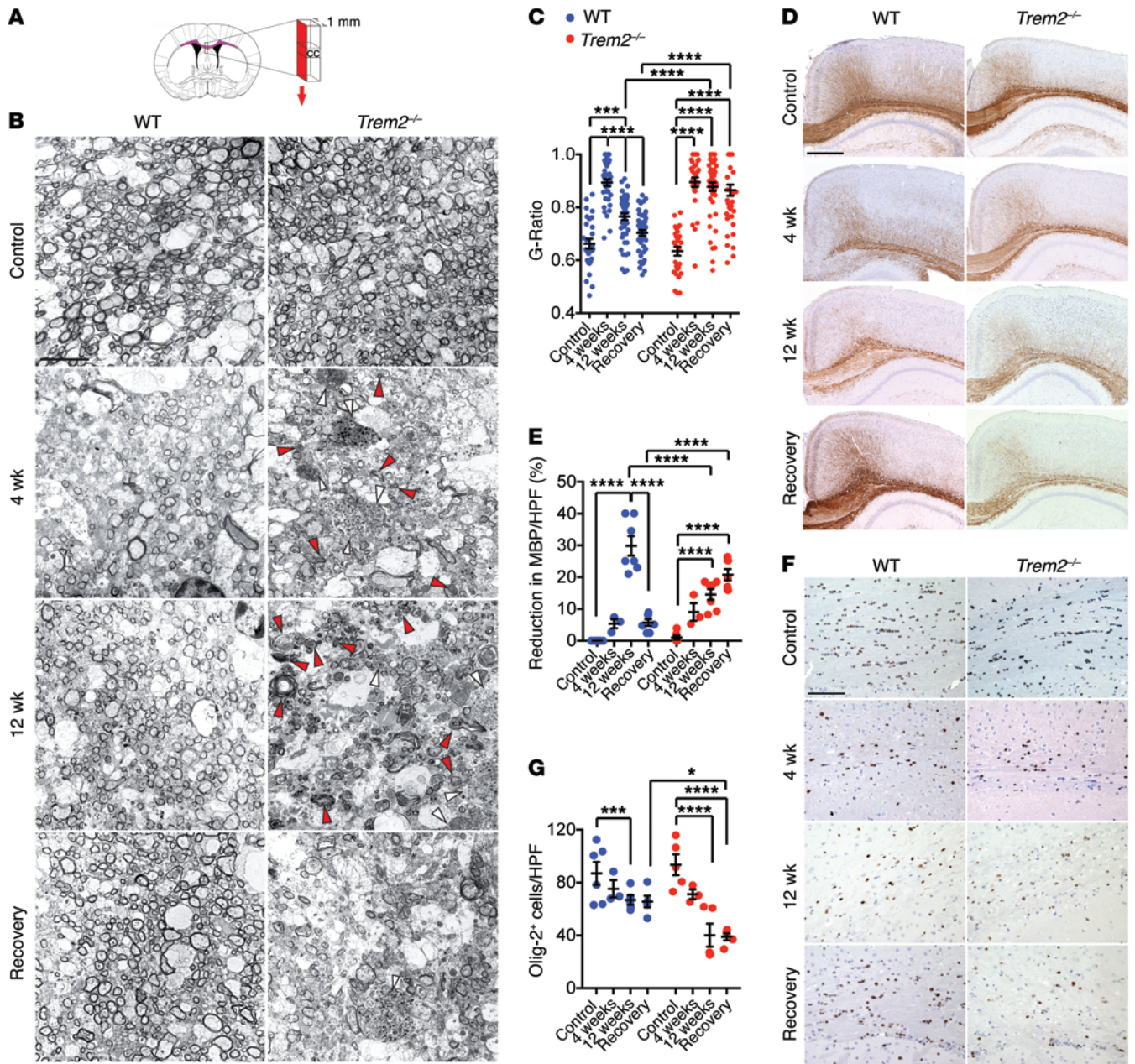


Figure 2. *Trem2*^{-/-} mice show impaired remyelination after cuprizone treatment. Mice were fed regular chow (control) or 0.2% cuprizone diet for 4 weeks, 12 weeks, or 12 weeks followed by 2 weeks of regular chow (recovery). (A–C) Myelination was assessed by TEM. (A) Strategy used for corpus callosum sectioning is indicated in red. (B) Representative images of corpus callosum in different treatments. Deposition of myelin debris (red arrowheads) and axonal spheroids (white arrowheads) is indicated in *Trem2*^{-/-} mice. (C) Demyelination and remyelination after cuprizone feeding is measured by changes in G ratios. (D–G) Brain sections were stained for MBP and Olig-2 to detect myelin and ODCs, respectively. Representative images for MBP (D) and Olig-2 staining (F). Percentage reduction of MBP reactivity in the total white matter area (E) and frequencies of Olig-2⁺ cells (G). **P* ≤ 0.05; ****P* ≤ 0.001; *****P* ≤ 0.0001, 2-way ANOVA. Original magnification, ×6000 (B); ×4 (D); ×20 (F). Scale bars: 5 μm (B); 500 μm (D); 100 μm (F). Data represent 2 to 3 mice (B and C) and 3 to 8 mice (D–G) per group. An average of 10 HPF per mouse were evaluated. Error bars represent mean ± SEM.

of cuprizone treatment, which progressively declined at 12 weeks and returned back to basal levels after recovery (Figure 3, A and B). In *Trem2*^{-/-} mice, microgliosis was less vigorous at 4 weeks, but persisted throughout the recovery phase (Figure 3, A and B). This unresolved microgliosis may be the consequence of a persisting accumulation of myelin debris. As previously observed in nontreated mice (see Figure 1), *Trem2*^{-/-} microglia in cuprizone-treated mice also exhibited dystrophic morphology,

as indicated by smaller cell bodies, as well as fragmentation, beading, and reduced ramification of microglial processes (Figure 3, C and D). These morphological changes suggested that *Trem2*^{-/-} microglia are dysfunctional.

TREM2 is required to activate microglial transcriptional programs for myelin clearance and repair. To further determine the impact of TREM2 deficiency on the microglial response to demyelination, we performed gene-expression profiling on microglia

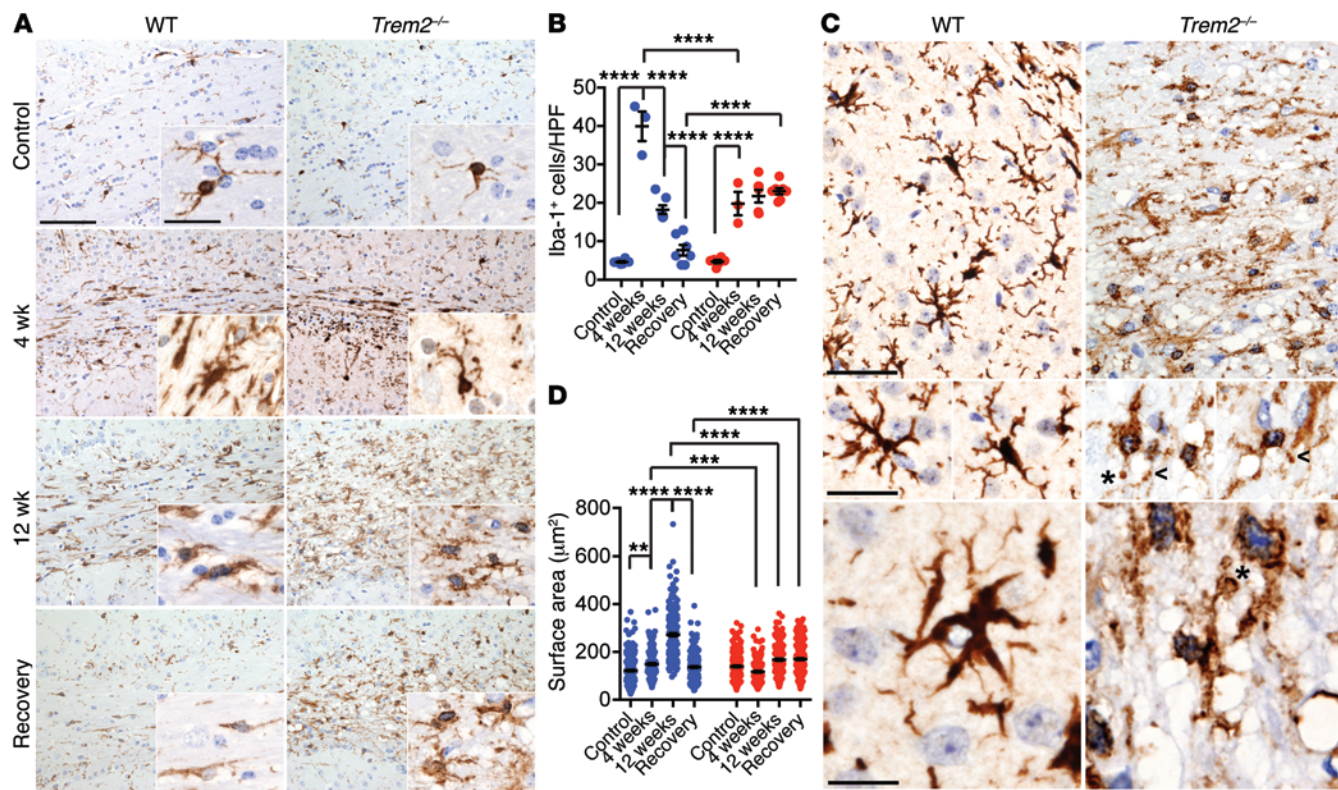


Figure 3. *Trem2* deficiency impairs microglial response to demyelination. Corpus callosum sections were stained with Iba-1 to detect microgliosis. (A) Representative images of Iba-1 staining. (B) Iba-1⁺ microglial frequencies per HPF. (C and D) Microglial morphology after cuprizone treatment. (C) Morphological assessment of WT and *Trem2*^{-/-} microglia after 12 weeks of cuprizone treatment. Fragmentation, beading (arrowheads), and spheroid formation (asterisks) are indicated. (D) Surface area of Iba-1⁺ microglia is quantified. ***P* ≤ 0.01; ****P* ≤ 0.001; *****P* ≤ 0.0001, 2-way ANOVA. Original magnification, ×20 (A); ×60 (A, insets; C, middle and bottom images); and ×40 (C, top images). Scale bars: 100 µm (A); 30 µm (C, middle and bottom images); 50 µm (C, top images). Data represent 3 to 8 mice (B) and 4 mice per group (D) for a total of 2 experiments. An average of 10 HPF per mouse were evaluated for B. An average of 50 cells in 10 HPF per mouse were evaluated for D. Error bars represent mean ± SEM.

isolated from brains of WT and *Trem2*^{-/-} mice that were either untreated (controls) or treated with cuprizone for 4 weeks (peak demyelination) or 12 weeks (prolonged demyelination and partial remyelination). A scatter plot of WT and *Trem2*^{-/-} microglia isolated from control mice demonstrated similar transcriptional profiles between the 2 genotypes, suggesting that TREM2 deficiency does not have a substantial impact on microglia in steady state (Figure 4A). We next determined the impact of cuprizone treatment on microglial gene transcription during the different stages of demyelination by comparing gene expression among WT mice. We found that a large set of microglial transcripts were upregulated (≥2-fold) at 4 weeks (Figure 4B); some of these transcripts remained elevated or were further upregulated at 12 weeks, whereas others were downregulated or returned to baseline at 12 weeks (Figure 4C). An additional set of transcripts were upregulated de novo at 12 weeks (Figure 4C). We further noticed that many genes had reduced expression at 12 weeks (Figure 4B). These transcripts included some that were initially upregulated at 4 weeks as well as others that were progressively reduced from the beginning of the treatment, but reached a marked downregulation (≤2-fold) only at 12 weeks (Figure 4C). Collectively, these data suggest that cuprizone treatment in WT mice activates a microglial transcriptional program early on, during the acute phase of demyelination. While some of

the induced genes persist and are further increased throughout cuprizone treatment, others are downregulated at late time points correlating with the ensuing remyelination.

To assess the impact of TREM2 deficiency on the cuprizone-induced transcriptional activation program, we visualized the gene signatures across the entire data set (WT and *Trem2*^{-/-} microglia). While most transcripts that were downregulated after cuprizone were not greatly affected by TREM2 deficiency, we noticed that many transcripts that were selectively increased at either 4 weeks, 12 weeks, or both 4 and 12 weeks were impaired in *Trem2*^{-/-} mice (Figure 4C). These included *Axl*, encoding a phagocytic receptor important for the uptake of myelin debris (39); *ApoE*, *Apoc1*, *Lpl*, and *Ch25h*, which specify key molecules for lipid transport and metabolism; and *Igfl*, which is a crucial growth factor for ODC differentiation. We also noticed that a group of transcripts that specifically upregulated at 12 weeks were affected by TREM2 deficiency. These encoded several inflammatory genes, such as *Il1b*, *Ifnb1*, *Il6*, and *Il12b*. Some of these transcriptional changes were further validated by quantitative PCR (qPCR) (Figure 4D). Together, these data indicate that during cuprizone-induced demyelination, TREM2 is required to activate microglia, prompting their response to myelin products and the induction of genes involved in myelin removal and repair and ODC maturation as well as inflammatory responses.

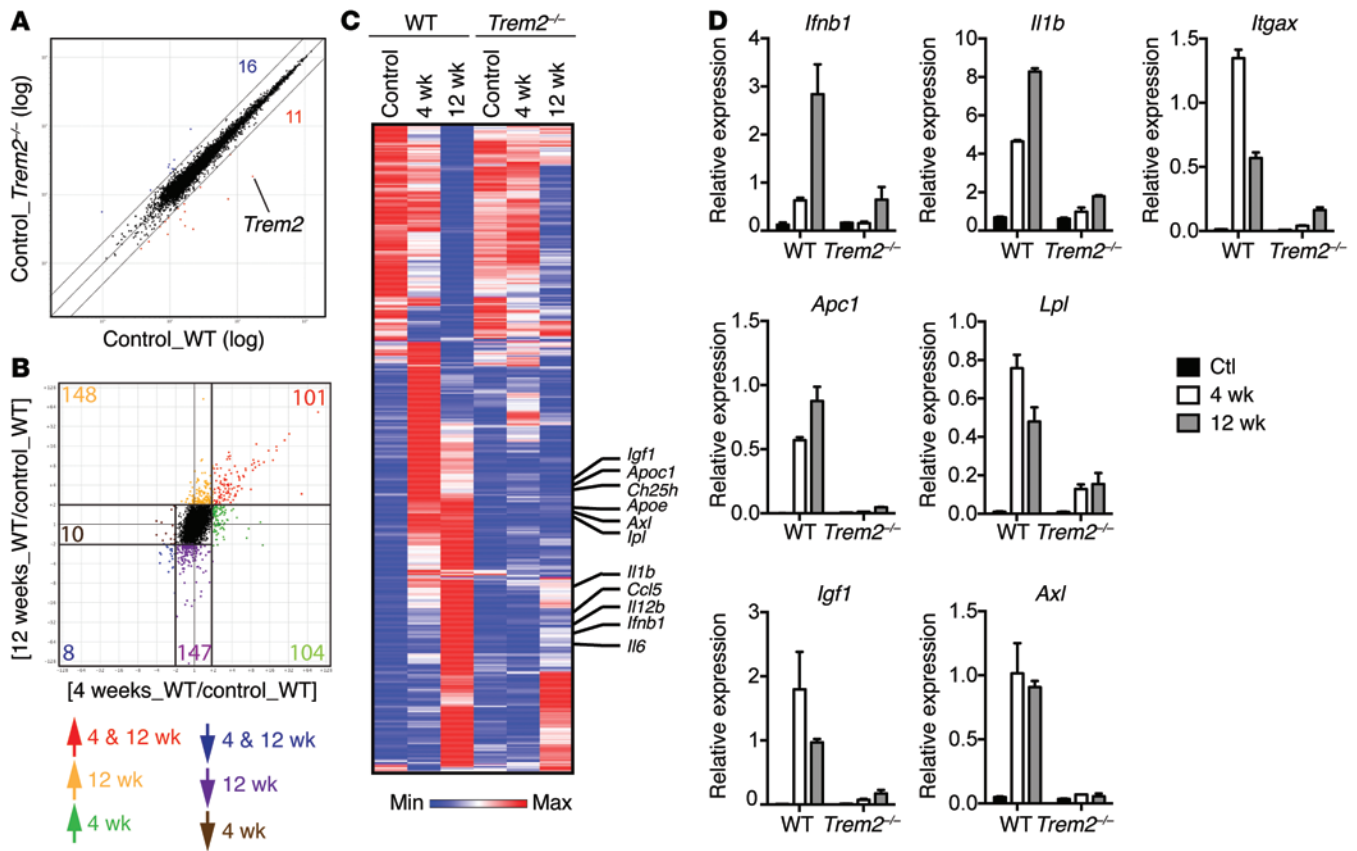


Figure 4. *Trem2*^{-/-} microglia fail to upregulate transcripts implicated in activation, phagocytosis, and lipid metabolism in response to demyelination.

Gene expression analyses of FACS-sorted WT and *Trem2*^{-/-} microglia from control mice and mice fed with cuprizone diet for 4 or 12 weeks. (A) Scatter plot shows comparison of WT and *Trem2*^{-/-} microglial transcriptomes in steady state. Numbers indicate transcripts that are differentially expressed (fold change ≥ 2) between WT and *Trem2*^{-/-} microglia. The *Trem2* transcript is indicated. (B) Transcriptional changes of WT microglia in response to cuprizone feeding for 4 weeks or 12 weeks compared with control (fold change ≥ 2 and ≤ 2). Numbers represent transcripts that are either differentially regulated at 4 weeks, 12 weeks, or both 4 and 12 weeks. (C) Heat map shows the expression of cuprizone-induced genes from B in WT and *Trem2*^{-/-} microglia. Selected transcripts are indicated. (D) Selected transcriptional changes (from C) were further validated by qPCR.

TREM2 detects lipid components of myelin. We next sought to determine the potential ligands that may activate TREM2 during demyelination. For this, we expressed mouse TREM2 (mTREM2) and DAP12 in a reporter cell line transfected with a chimeric gene encoding the GFP under the control of nuclear factor of activated T cells-responsive (NFAT-responsive) elements. Engagement of the mTREM2/DAP12 complex in these cells leads to mobilization of intracellular Ca²⁺, which triggers GFP expression. Since TREM2 was shown to detect polyanions and phospholipids (6, 8), we tested lipid components of myelin. We initially incubated mTREM2-DAP12 reporter cells in wells coated with crude lipid extracts obtained from normal mouse brains. Myelin lipids induced GFP expression, which was blocked by the addition of anti-TREM2 mAb (Figure 5, A and B). Control mTREM1-DAP12 reporter cells or parental reporter cells were not activated. Thus, myelin components can trigger TREM2 signaling. To further investigate the specificity of TREM2, we incubated mTREM2-DAP12 reporter cells with purified lipid components of myelin, such as sulfatide, cerebroside, sphingomyelin, and various phospholipids. Many of these lipidic components stimulated TREM2 signaling, with the exception of cerebroside (Figure 5C). These results suggest that TREM2

may detect myelin injury by sensing some of the glycolipids and phospholipids that compose myelin and may be exposed during myelin damage.

Discussion

It has been established that TREM2 is expressed in brain-resident microglia (1, 2, 35) and that TREM2 deficiency causes demyelinating NHD (1). However, the function of TREM2 in brain-resident microglia in vivo and the mechanisms underlying NHD demyelination are poorly understood. Our study demonstrates that TREM2 is a sensor for brain lipidic components that promotes microglial fitness and expansion during normal aging. Indeed, TREM2 deficiency hindered the accumulation of microglia during aging, particularly in the corpus callosum, which is rich in myelin that may provide a major stimulus for TREM2 signaling. Microglia were also defective in the cerebellum and hippocampus, which contain less myelin than the corpus callosum; however, no defect was observed in the cortex. The variable impact of TREM2 signaling in distinct brain regions may depend on their myelin content, the presence of alternative TREM2 ligands, the level of TREM2 expression, and the presence of other receptor-ligand interactions that can com-

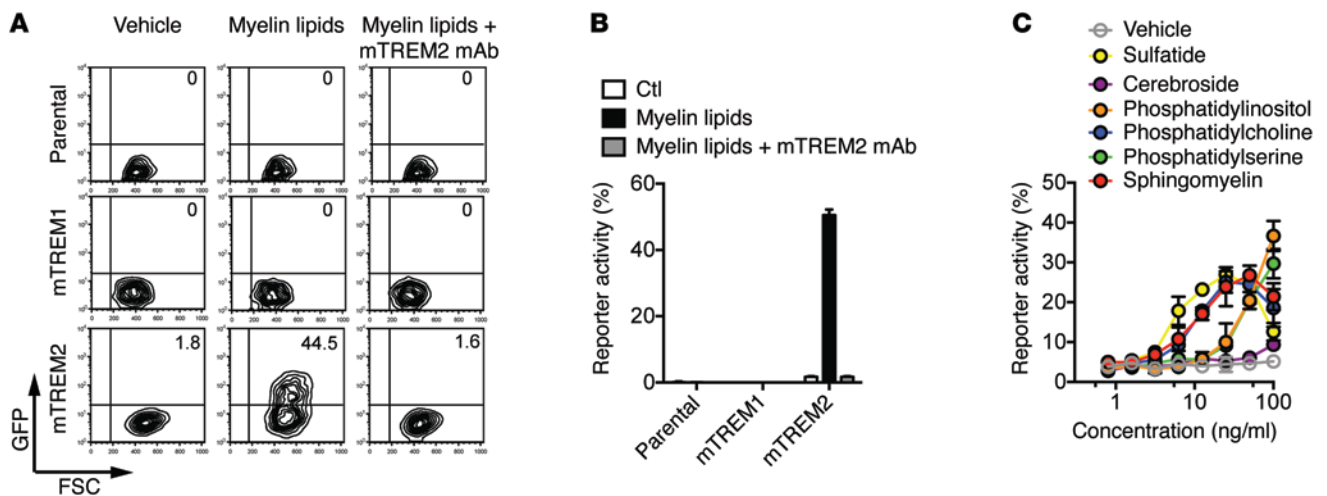


Figure 5. Myelin lipids activate mTREM2-NFAT-GFP reporter cells. (A and B) mTREM1, mTREM2, and parental reporter cells were stimulated with crude myelin lipids purified from brains of WT mice with or without the addition of anti-mTREM2 mAb. (A) Representative data show GFP expression examined by flow cytometry 16 hours after stimulation. (B) Results from 3 independent experiments are quantified. Ctl, control. (C) mTREM2 reporter cells were stimulated overnight with various lipids at indicated concentrations, and GFP expression was measured by flow cytometry. Data are representative of 2 independent experiments. Error bars represent mean \pm SEM.

compensate for the lack of TREM2. Interestingly, while the reduction of microglia in *Trem2*^{-/-} mice was not paralleled by obvious pathology, a complete defect in TREM2 function appears sufficient to cause NHD in humans. Since the mTREM gene complex contains more genes than its human counterpart (10), it is possible that TREM2 deficiency in mice is partially compensated by other as-yet-uncharacterized TREM receptors. Alternatively, the development of NHD may require not only a genetically inherited TREM2 deficiency, but also environmental stimuli that do not occur in mice in the steady state.

We used the cuprizone model to expose a potential function for TREM2 during demyelination in mice. In this model, which predominantly affects the corpus callosum, TREM2 was required for microglial response to prolonged demyelination and induction of coordinated transcriptional programs for removal of damaged myelin sheaths and secretion of trophic factors that support ODC differentiation/survival. A defect in TREM2 function resulted in accumulation of myelin debris, which has been shown to inhibit ODC precursor cell differentiation and remyelination (40). Moreover, accumulating myelin debris may provide continued recruitment signals to microglia, which would explain the maintenance of microglial numbers in the corpus callosum of *Trem2*^{-/-} mice throughout cuprizone treatment, including the recovery phase.

We showed that TREM2 signaling sustains multiple microglial transcriptional programs that do not fit the conventional M1/M2 paradigm (41). One of these programs leads to the expression of genes induced by IFN- α/β and inflammatory cytokines, consistent with previous reports (42, 43). Most likely, myelin degradation products enter the microglia and engage innate sensors of damage-associated molecular patterns, which trigger the IFN- α/β , NF- κ B, and inflammasome pathways. Another transcriptional program promotes lipid and cholesterol uptake, transport, and processing. The expression of genes for lipid processing is consistent with previous studies

(44, 45) and is most likely a consequence of microglia uptake of lipoproteins released during myelin damage. Finally, activated microglia express genes that encode chemokines that attract other glial cells and trophic factors, such as IGF1, that promote differentiation and maturation of ODCs, which in turn mediate remyelination. How TREM2 mediates the induction of these multiple gene programs remains unclear. Given that TREM2 and DAPI2 promote macrophage survival in the presence of limited concentrations of CSF-1 (11, 46) and that CSF-1 production in the brain may be limited, especially during neuronal and glial damage, TREM2-deficient microglia may be unfit overall and hence dysfunctional; they simply may not be sufficiently robust to activate the multiple programs required for an effective response to myelin damage. Alternatively, TREM2 may be required as a coreceptor for other activating receptors. As DAPI2 is located in lipid rafts, engagement of TREM2 may induce aggregation and mobilization of multiple receptors to lipid rafts (47), thereby facilitating their clustering and activation of multiple signaling pathways.

Very recent studies have shown that individuals heterozygous for a rare variant of TREM2, R47H, have high risk for developing Alzheimer disease (AD) (34, 48, 49). The same variant is a risk factor for Parkinson's disease (PD) and sporadic amyotrophic lateral sclerosis (ALS) (50, 51). The R47H variant impairs TREM2 lipid recognition (52). Thus, it is possible that the TREM2-dependent mechanisms underlying demyelination, AD, PD, and ALS are similar. We have shown that TREM2-deficient microglia fail to remove damaged myelin; similarly, TREM2 may be required for an effective microglia response to and clearance of β -amyloid plaques and other aggregated prion-like proteins. TREM2 may also be required to sustain microglial trophic function, which has been shown to contribute to neuronal homeostasis in the aging brain (37). Interestingly, it was reported that microglial TREM2 expression is reduced in aged mice (37). It is possible that a progressive decline in TREM2

expression may also occur during aging in certain areas of the human brain, curtailing microglial numbers and the microglial response to the breakdown of myelin, glial cells, and neurons, which would create fertile ground for neurodegeneration. It will be essential to quantify TREM2 expression in different areas of the mouse and human brain at different ages in future studies.

Our TREM2 reporter assays suggest that mTREM2 may bind a broad array of glycolipids and phospholipids, which may be exposed on damaged myelin sheaths as well as on dying glial cells and neurons. We recently demonstrated that human TREM2 detects a similarly broad range of anionic and zwitterionic lipid ligands (52). However, because cerebroside did not activate mTREM2 signaling, TREM2 ligands may have distinct structural constraints that remain to be defined. It is also unclear whether TREM2 binds lipid components within lipoproteins, exosomes, apoptotic cells, or other supramolecular structures. Recent studies have demonstrated that TREM2 is released from the surface of cells through the consecutive action of ADAM10 and γ -secretase (53, 54). Thus, soluble TREM2 might also contribute to transport, delivery, or metabolism of myelin products. In conclusion, our data demonstrate that TREM2 is a lipid sensor that transmits intracellular signals that promote the overall fitness of microglia during aging as well as their ability to respond to prolonged demyelination. The cuprizone treatment of *Trem2*^{-/-} mice presented here partially recapitulates the pathology of human NHD. Future studies will determine whether impairment of TREM2 function affects other demyelinating and neurodegenerative diseases.

Methods

Mice and cuprizone treatment. Generation of *Trem2*^{-/-} mice has been previously described (13). All mice were bred and housed in the same animal facility. Cuprizone was purchased from Sigma-Aldrich (catalog 14690) and sent to Harlan Laboratories to produce a diet containing 0.2% cuprizone.

Immunohistochemistry. Paraffin-embedded brain sections (2 μ m thick) were dewaxed, rehydrated, and treated with 0.3% H₂O₂/methanol to block endogenous peroxidase. Heat-induced antigen retrieval was obtained by microwave treatment or incubation in a thermostatic bath using 1 mM EDTA-Tris-HCl buffer, pH 8.0. Sections were stained with rat anti-MBP mAb (clone AB980, Chemicon), rabbit anti-Iba-1 polyclonal antibody (Wako Chemicals, catalog 019-19741), and rabbit anti-Olig-2 polyclonal antibody (Life Technologies, catalog P21954). Stainings were revealed by Real EnVision Rabbit HRP Labelled Polymer System (Dako) and Rat on Mouse HRP Polymer Kit (Biocare Medical) using 3,3'-diaminobenzidine tetrahydrochloride (0.05%) as a chromogen and hematoxylin as counterstaining. Demyelination was evaluated with a morphometric method by measuring the percentage of demyelinated area over the total area of corpus callosum. A Nikon Eclipse 50i microscope was used to count cells. Changes in MBP and microglia surface areas were measured by an Olympus DP70 camera mounted on an Olympus Bx60 microscope, using CellF Imaging software (Soft Imaging System GmbH).

TEM. TEM was performed as previously described (55). In brief, brains were perfused with formalin and fixed in formalin overnight. Dissected tissues (1 mm in thickness) were postfixed in buffered OsO₄,

dehydrated in graded alcohol solutions and propylene, embedded in Epon, and examined by light microscopy after toluidine blue staining. Thin sections cut onto Formvar-coated slot grids and stained with uranyl acetate and lead citrate were examined and recorded with a JEOL 1200 electron microscope. G ratios were determined by measuring the ratio of circumference of axon over myelin using ImageJ (<http://imagej.nih.gov/ij/>).

Gene expression analysis and qPCR. Brains from 3 mice were dissected and dissociated using a neuronal tissue dissociation kit (Miltenyi Biotec). Microglia were enriched using mouse CD45 beads (Miltenyi Biotec) followed by FACS sorting of CD45^{lo}CD11b⁺ cells using CD45-eFluor450 (30F-11, eBioscience) and CD11b-APC (M1/70, BD Biosciences — Pharmingen). Astrocytes and ODC progenitors were FACS sorted from the CD45⁻ fraction using ASCA-1-PE antibody (ASCA-1) and A2B5-APC antibody (105HB29), respectively (Miltenyi Biotec). A FACSaria II (BD) was used for all FACS-sorting experiments, with greater than 99% purity achieved. Cells were sorted directly into RLT buffer, and RNA was extracted using an RNeasy Micro Kit (QIAGEN). For microarray analyses, hybridization (Affymetrix MoGene 1.0 ST array) and data processing were performed at the Washington University Genome Center. Robust multi-array average (RMA) normalization was used, and genes were prefiltered for expression value of 120 or more. Scatter plots and dot plots were produced using the Multiplot module of GenePattern (Broad Institute). Venn diagrams and heat map were generated from a selected gene list using GENE-E (Broad Institute). The expression of selected gene list was further validated by qPCR using a SYBR Green PCR Master Mix (Bio-Rad) and amplified on an ABI7000 machine (Applied Biosystems). qPCR primers used in this study are listed in Supplemental Table 1.

Accession numbers. All original microarray data were deposited in the NCBI's Gene Expression Omnibus (GEO GSE66926).

Reporter assay. 43.1 reporter T cells (56) were stably transfected with mTREM2 or mTREM1 and DAPI2 cDNAs. A monoclonal anti-murine TREM2 antibody (13) was used to block TREM2 signaling. To extract myelin lipids, myelin vesicles were generated as previously described (57). Briefly, brain from a WT mouse was homogenized with a Dounce homogenizer and resuspended in 0.25 M sucrose solution, followed by centrifugation onto a sucrose gradient. Crude lipids were extracted from myelin vesicles with methanol. Myelin lipids or other purified lipids dissolved in methanol were coated onto a high-absorbent plate (catalog 442404, Thermo Scientific) and incubated at room temperature for 4 hours to allow methanol evaporation. Reporter cells were added to lipid-coated wells or solvent-treated control wells and assessed after overnight incubation. Reporter activity (%) was defined as percentage of GFP⁺ cells in lipid-coated wells subtracted from background (percentage of GFP⁺ cells in solvent-treated wells).

Statistics. Data in figures are presented as mean \pm SEM. All statistical analysis was performed using Prism (GraphPad). Statistical analysis to compare the mean values for multiple groups was performed using 1-way or 2-way ANOVA with correction for multiple comparisons. Comparison of 2 groups was performed using a 2-tailed unpaired *t* test (Mann Whitney *U* test). Values were accepted as significant at *P* \leq 0.05.

Study approval. All animal studies were approved by the Washington University Animal Studies Committee.

Acknowledgments

P.L. Poliani is supported by Fondazione Cariplo. Y. Wang is supported by the Lilly Innovation Fellowship Award (Eli Lilly and Company). Y. Yamanishi is supported by a postdoctoral fellowship for research abroad from the Japan Society for the Promotion of Science. M. Colonna is supported by Knight Alzheimer's Disease Research Center pilot grant P50 AG005681-30 and the Cure Alzheimer's Fund. We thank the Genome Technology Access Center in the Department of Genetics (Washington University School of Medicine) for help with gene expression analysis. We

thank Robert E. Schmidt, Karen Green, and the Morphology and Metabolic Analysis Core (Diabetes Research Center, Washington University School of Medicine, grant no. NIH DK020579) for assistance with TEM analyses. We thank Takashi Saito (RIKEN) for providing the NFAT-GFP reporter cells.

Address correspondence to: Marco Colonna, Washington University School of Medicine, Department of Pathology and Immunology, 660 S. Euclid Ave., Box 8118, St. Louis, Missouri 63110, USA. Phone: 314.362.0367; E-mail: mcolonna@pathology.wustl.edu.

- Paloneva J, et al. Mutations in two genes encoding different subunits of a receptor signaling complex result in an identical disease phenotype. *Am J Hum Genet.* 2002;71(3):656–662.
- Schmid CD, et al. Heterogeneous expression of the triggering receptor expressed on myeloid cells-2 on adult murine microglia. *J Neurochem.* 2002;83(6):1309–1320.
- Correale C, et al. Bacterial sensor triggering receptor expressed on myeloid cells-2 regulates the mucosal inflammatory response. *Gastroenterology.* 2013;144(2):346–356 e343.
- Bouchon A, Hernandez-Munain C, Cella M, Colonna M. A DAP12-mediated pathway regulates expression of CC chemokine receptor 7 and maturation of human dendritic cells. *J Exp Med.* 2001;194(8):1111–1122.
- Daws MR, Lanier LL, Seaman WE, Ryan JC. Cloning and characterization of a novel mouse myeloid DAP12-associated receptor family. *Eur J Immunol.* 2001;31(3):783–791.
- Daws MR, Sullam PM, Niemi EC, Chen TT, Tchao NK, Seaman WE. Pattern recognition by TREM-2: binding of anionic ligands. *J Immunol.* 2003;171(2):594–599.
- N'Diaye EN, et al. TREM-2 (triggering receptor expressed on myeloid cells 2) is a phagocytic receptor for bacteria. *J Cell Biol.* 2009;184(2):215–223.
- Cannon JP, O'Driscoll M, Litman GW. Specific lipid recognition is a general feature of CD300 and TREM molecules. *Immunogenetics.* 2012;64(1):39–47.
- Lanier LL. DAP10- and DAP12-associated receptors in innate immunity. *Immunol Rev.* 2009;227(1):150–160.
- Ford JW, McVicar DW. TREM and TREM-like receptors in inflammation and disease. *Curr Opin Immunol.* 2009;21(1):38–46.
- Otero K, et al. Macrophage colony-stimulating factor induces the proliferation and survival of macrophages via a pathway involving DAP12 and beta-catenin. *Nat Immunol.* 2009;10(7):734–743.
- Peng Q, Long CL, Malhotra S, Humphrey MB. A physical interaction between the adaptor proteins DOK3 and DAP12 is required to inhibit lipopolysaccharide signaling in macrophages. *Sci Signal.* 2013;6(289):ra72.
- Turnbull IR, et al. Cutting edge: TREM-2 attenuates macrophage activation. *J Immunol.* 2006;177(6):3520–3524.
- Hamerman JA, Jarjoura JR, Humphrey MB, Nakamura MC, Seaman WE, Lanier LL. Cutting edge: inhibition of TLR and FcR responses in macrophages by triggering receptor expressed on myeloid cells (TREM)-2 and DAP12. *J Immunol.* 2006;177(4):2051–2055.
- Verloes A, Maquet P, Sadzot B, Vivario M, Thiry A, Franck G. Nasu-Hakola syndrome: polycystic lipomembranous osteodysplasia with sclerosing leucoencephalopathy and presenile dementia. *J Med Genet.* 1997;34(9):753–757.
- Simons M, Lyons DA. Axonal selection and myelin sheath generation in the central nervous system. *Curr Opin Cell Biol.* 2013;25(4):512–519.
- Prinz M, Priller J, Sisodia SS, Ransohoff RM. Heterogeneity of CNS myeloid cells and their roles in neurodegeneration. *Nat Neurosci.* 2011;14(10):1227–1235.
- Ransohoff RM, Cardona AE. The myeloid cells of the central nervous system parenchyma. *Nature.* 2010;468(7321):253–262.
- Miron VE, et al. M2 microglia and macrophages drive oligodendrocyte differentiation during CNS remyelination. *Nat Neurosci.* 2013;16(9):1211–1218.
- Kaifu T, et al. Osteopetrosis and thalamic hypomyelination with synaptic degeneration in DAP12-deficient mice. *J Clin Invest.* 2003;111(3):323–332.
- Takahashi K, Rochford CD, Neumann H. Clearance of apoptotic neurons without inflammation by microglial triggering receptor expressed on myeloid cells-2. *J Exp Med.* 2005;201(4):647–657.
- Takahashi K, Prinz M, Stagi M, Chechneva O, Neumann H. TREM2-transduced myeloid precursors mediate nervous tissue debris clearance and facilitate recovery in an animal model of multiple sclerosis. *PLoS Med.* 2007;4(4):e124.
- Greter M, Merad M. Regulation of microglia development and homeostasis. *Glia.* 2013;61(1):121–127.
- Gomez Perdiguero E, Schulz C, Geissmann F. Development and homeostasis of “resident” myeloid cells: the case of the microglia. *Glia.* 2013;61(1):112–120.
- Ajami B, Bennett JL, Krieger C, Tetzlaff W, Rossi FM. Local self-renewal can sustain CNS microglia maintenance and function throughout adult life. *Nat Neurosci.* 2007;10(12):1538–1543.
- Mildner A, et al. Microglia in the adult brain arise from Ly-6ChiCCR2+ monocytes only under defined host conditions. *Nat Neurosci.* 2007;10(12):1544–1553.
- Matsushima GK, Morell P. The neurotoxicant, cuprizone, as a model to study demyelination and remyelination in the central nervous system. *Brain Pathol.* 2001;11(1):107–116.
- Gudi V, Gingele S, Skripuletz T, Stangel M. Glial response during cuprizone-induced de- and remyelination in the CNS: lessons learned. *Front Cell Neurosci.* 2014;8:73.
- Mouton PR, et al. Age and gender effects on microglia and astrocyte numbers in brains of mice. *Brain Res.* 2002;956(1):30–35.
- Tremblay ME, Zettel ML, Ison JR, Allen PD, Majewska AK. Effects of aging and sensory loss on glial cells in mouse visual and auditory cortices. *Glia.* 2012;60(4):541–558.
- Damani MR, Zhao L, Fontainhas AM, Amaral J, Fariss RN, Wong WT. Age-related alterations in the dynamic behavior of microglia. *Aging Cell.* 2011;10(2):263–276.
- Kondo A, Nakano T, Suzuki K. Blood-brain barrier permeability to horseradish peroxidase in twitcher and cuprizone-intoxicated mice. *Brain Res.* 1987;425(1):186–190.
- Sessa G, et al. Distribution and signaling of TREM2/DAP12, the receptor system mutated in human polycystic lipomembranous osteodysplasia with sclerosing leucoencephalopathy dementia. *Eur J Neurosci.* 2004;20(10):2617–2628.
- Guerreiro R, et al. TREM2 variants in Alzheimer's disease. *N Engl J Med.* 2013;368(2):117–127.
- Butovsky O, et al. Identification of a unique TGF- β -dependent molecular and functional signature in microglia. *Nat Neurosci.* 2014;17(1):131–143.
- Jiang T, et al. Upregulation of TREM2 ameliorates neuropathology and rescues spatial cognitive impairment in a transgenic mouse model of Alzheimer's disease. *Neuropsychopharmacology.* 2014;39(13):2949–2962.
- Hickman SE, et al. The microglial sensome revealed by direct RNA sequencing. *Nat Neurosci.* 2013;16(12):1896–1905.
- Gudi V, et al. Spatial and temporal profiles of growth factor expression during CNS demyelination reveal the dynamics of repair priming. *PLoS One.* 2011;6(7):e22623.
- Hoehn HJ, Kress Y, Sohn A, Brosnan CF, Bourdon S, Shafiq-Zagardo B. Axl $^{-/-}$ mice have delayed recovery and prolonged axonal damage following cuprizone toxicity. *Brain Res.* 2008;1240:1–11.
- Kotter MR, Li WW, Zhao C, Franklin RJ. Myelin impairs CNS remyelination by inhibiting oligodendrocyte precursor cell differentiation. *J Neurosci.* 2006;26(1):328–332.
- Wen H, et al. Fatty acid-induced NLRP3-ASC inflammasome activation interferes with insulin signaling. *Nat Immunol.* 2011;12(5):408–415.
- Schmidt H, et al. Type I interferon receptor signaling is induced during demyelination while its function for myelin damage and repair is redundant. *Exp Neurol.* 2009;216(2):306–311.

43. Mason JL, Suzuki K, Chaplin DD, Matsushima GK. Interleukin-1 β promotes repair of the CNS. *J Neurosci*. 2001;21(18):7046-7052.
44. Olah M, et al. Identification of a microglia phenotype supportive of remyelination. *Glia*. 2012;60(2):306-321.
45. Voss EV, et al. Characterisation of microglia during de- and remyelination: can they create a repair promoting environment? *Neurobiol Dis*. 2012;45(1):519-528.
46. Otero K, et al. TREM2 and beta-catenin regulate bone homeostasis by controlling the rate of osteoclastogenesis. *J Immunol*. 2012;188(6):2612-2621.
47. Lingwood D, Simons K. Lipid rafts as a membrane-organizing principle. *Science*. 2010;327(5961):46-50.
48. Jonsson T, et al. Variant of TREM2 associated with the risk of Alzheimer's disease. *N Engl J Med*. 2013;368(2):107-116.
49. Zhang B, et al. Integrated systems approach identifies genetic nodes and networks in late-onset Alzheimer's disease. *Cell*. 2013;153(3):707-720.
50. Cady J, et al. TREM2 variant p.R47H as a risk factor for sporadic amyotrophic lateral sclerosis. *JAMA Neurol*. 2014;71(4):449-453.
51. Rayaprolu S, et al. TREM2 in neurodegeneration: evidence for association of the p.R47H variant with frontotemporal dementia and Parkinson's disease. *Mol Neurodegener*. 2013;8:19.
52. Wang Y, et al. TREM2 lipid sensing sustains the microglial response in an Alzheimer's disease model. *Cell*. 2015;160(6):1061-1071.
53. Wunderlich P, Glebov K, Kemmerling N, Tien NT, Neumann H, Walter J. Sequential proteolytic processing of the triggering receptor expressed on myeloid cells-2 (TREM2) protein by ectodomain shedding and gamma-secretase-dependent intramembranous cleavage. *J Biol Chem*. 2013;288(46):33027-33036.
54. Kleinberger G, et al. TREM2 mutations implicated in neurodegeneration impair cell surface transport and phagocytosis. *Sci Transl Med*. 2014;6(243):243ra286.
55. Malik I, et al. Disrupted membrane homeostasis and accumulation of ubiquitinated proteins in a mouse model of infantile neuroaxonal dystrophy caused by PLA2G6 mutations. *Am J Pathol*. 2008;172(2):406-416.
56. Ohtsuka M, et al. NFAM1, an immunoreceptor tyrosine-based activation motif-bearing molecule that regulates B cell development and signaling. *Proc Natl Acad Sci U S A*. 2004;101(21):8126-8131.
57. Sedzik J, Blaurock AE. Myelin vesicles: what we know and what we do not know. *J Neurosci Res*. 1995;41(2):145-152.